Linear Behavior of Carbon Nanotube Diameters with Growth Temperature

ARTICLE *in* THE JOURNAL OF PHYSICAL CHEMISTRY C · AUGUST 2010

Impact Factor: 4.77 · DOI: 10.1021/jp105815u

4 AUTHORS, INCLUDING:

Michael P Siegal
Sandia National Laboratories
170 PUBLICATIONS **3,660** CITATIONS
SEE PROFILE

P. P. Provencio
University of New Mexico
153 PUBLICATIONS **4,254** CITATIONS
SEE PROFILE

Linear Behavior of Carbon Nanotube Diameters with Growth Temperature

Michael P. Siegal,* Donald L. Overmyer, Paula P. Provencio, and David R. Tallant

Sandia National Laboratories, Albuquerque, New Mexico 87185

Received: June 23, 2010; Revised Manuscript Received: July 30, 2010

High crystalline quality single- and multiwalled carbon nanotubes (CNTs) grow using thermal chemical vapor deposition (CVD) at temperatures ranging from 530 to 630 °C. Using identical Ni catalyst layers and a constant CO reduction annealing process at 600 °C, the number of walls in the resulting CNTs increases linearly from one to eight over this growth temperature range. The highest temperature used in the growth process appears to control the resulting inner core diameter, which is ∼1 nm for all CNTs grown ≤ 610 °C, near the CO reduction anneal used for all the samples. The corresponding CNT outer diameters also increase linearly from 1 to 5 nm up to 610 °C. Using growth temperatures measurably higher than that of the reduction anneal results in both larger inner and outer diameters, inferring that the Ni catalyst islands grow with increasing temperature. These results suggest that independent control of the number of walls and the inner core diameter in CNTs is possible.

Introduction

Many intensive studies have been published on the growth and characterization of multiwalled carbon nanotubes (CNT), primarily by catalyst−supported chemical vapor deposition (CVD). Although the CVD methods vary somewhat, ranging from high-vacuum, hot-filament, and microwave-assisted to simple ambient-pressure thermal processes, most reports result in multiwalled CNTs with diameters > 20 nm, compared with ≤ 3 nm for single-walled CNTs. The structure of these large-diameter multiwalled CNTs tends to be highly disordered with many structural defects, including kinks, bends, wall breaks, and bamboo structures.[1−6] The advent of such structural disorder may result from the high growth rates of many of the CVD processes used; however, this is not known for certain.[7]

We reported the growth of multiwalled CNTs with highly controlled diameters, ranging from 7 to 350 nm, using a thermal CVD process over a temperature range of 630−790 °C.[8] Furthermore, we showed how the CNT site density can be controlled over 4 orders of magnitude by careful selection of the hydrocarbon feed gas in combination with the residual stress of the metal catalyst films.[9] Briefly, we demonstrated that the CNT diameter increases with increasing growth temperature. The lowest growth temperature used in that study was 630 °C and resulted in ∼7 nm diameter CNTs. This thermal CVD method yields CNTs that are relatively straight and uniform in diameter along their lengths compared to those grown by other CVD methods.

The importance of the structural features and chemical state of the metal catalyst clusters is generally assumed but is only recently becoming better understood.[10−12] The most commonly used catalysts for CNT growth are Ni, Co, and Fe, and each typically is pretreated in some type of high-temperature anneal in a reducing atmosphere to eliminate oxides and make the catalyst more chemically reactive with the CVD hydrocarbon feed gas. For instance, Hoffman et al. show that 1 nm thick Ni films deposited onto SiO_2-coated Si become small islands when heated in the presence of NH_3 reducing gas at temperatures as low as 480 °C with a size distribution centered near 5 nm diameters.[13] At the higher reducing temperature of 615 °C, the islands are somewhat larger with a wider size distribution. They hypothesize that the larger catalyst island sizes lead to larger diameter CNTs.

Nessim et al. show a similar result using Fe catalyst films with H_2 reducing anneals at 770 °C.[14] The reduction annealing time is varied to control Fe particle sizes that correlate with the resulting CNT diameter. Shorter times at this relatively high reduction temperature lead to smaller Fe sizes, which, in turn, yield smaller diameter CNTs than longer reduction anneals. Kim et al. essentially confirm this result with studies of CNT growth using H_2 reduction anneals at 750 °C for 1 nm thick Fe catalyst films: longer time treatments result in a greater wall diameter and size distribution.[15]

This paper reports CNT growth at temperatures as low as to 530 °C and finds that the trend of smaller diameters continues. Here, we characterize the structure of CNTs with greater detail as a function of growth temperature, identifying inner and outer diameters of CNTs, the number of graphene cylindrical walls in these tubes, and the types of structural disorder that occurs, including whether or not graphitic carbon exists in the CNTs. These structural measurements will be correlated with detailed Raman spectra for these films to bring greater understanding to the chemical bonding nature that exists in these multiwalled CNTs grown as films.

Experimental Section

Materials. CNT growth is described elsewhere.[8] Briefly, Si(100) wafers are cleaned with an HF dip, followed by a DI water rinse, and loaded into an rf sputter deposition system. First, a 50 nm thick W diffusion barrier is deposited, followed by a 2.5 nm thick Ni catalyst layer through an Al foil shadow mask with ∼1 mm diameter holes, resulting in 9 dots/cm^2 of Ni/W metallization on the Si(100) wafer. The W diffusion barrier prevents unwanted Ni−silicide formation. The dots prevent spallation from stresses arising during thermal CVD growth between W and Si due to their different coefficients of thermal expansion. The sputter conditions used for both W and

* To whom correspondence should be addressed. E-mail: mpsiega@sandia.gov.

10.1021/jp105815u
Published on Web 08/19/2010

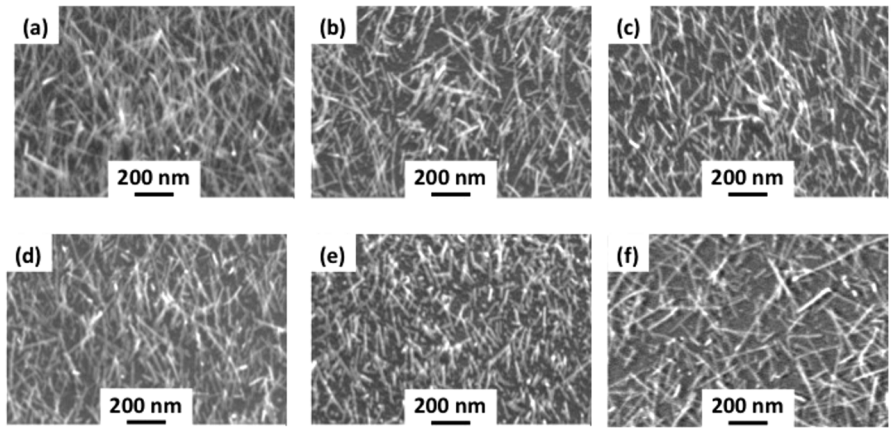

Figure 1. SEM images for CNTs grown using a 1.5 nm thick Ni catalyst film on 50 nm thick W-coated Si(100) substrates at (a) 530, (b) 550, (c) 570, (d) 590, (e) 610, and (f) 630 °C.

Ni deposition minimize the residual stress of each layer, which maximizes the CNT nucleation site density.[9]

Reaction. Samples are placed in a quartz tube furnace and heated to 600 °C for 1 h in flowing CO at atmospheric pressure (~620 Torr in Albuquerque, NM) to reduce the Ni layer. Following this oxygen reducing anneal, the ambient is flushed with N_2 and the temperature ramped to the CNT growth temperature in 15 min, ranging from 530 to 630 °C for this study. Next, the tube is flushed with the CVD growth carbon source at ambient pressure (8% C_2H_2:92% N_2) and held at the growth temperature for 15 min. Acetylene has a high heat of formation and is a very reactive hydrocarbon feed gas, yielding high densities of CNTs on surfaces.[9] Finally, the C_2H_2 flow is halted and the samples are furnace-cooled to room temperature in N_2.

Characterization. Scanning electron microscopy (SEM) determines the presence of CNTs on a given substrate, along with their overall distribution and morphologies. High-resolution transmission electron microscopy (TEM) elucidates the nanostructural nature of the individual nanotubes produced at different growth temperatures. Samples are prepared for TEM by lightly agitating them in acetone to remove CNTs from the Si substrate and get them into solution. Drops of solution are then deposited onto a holey carbon TEM grid for analysis. Raman spectroscopy, using 514 nm incident light, is used to analyze the nature of the carbon−carbon bonding of the CNT films as a function of growth temperature.

Results

Electron Microscopy. Previous work using the same growth method found that CNT diameters increase exponentially from 5 to 300 nm using 4 nm thick Ni catalyst films with increasing growth temperatures from 630 to 790 °C.[8] High-resolution TEM studies determined that only samples grown at 630 °C were clean multiwalled CNTs. Higher temperature growth yields structures consisting essentially of the CNT grown at 630 °C surrounded in an amorphous carbon sheath that increased exponentially in thickness with increasing growth temperature.[16] This present work extends those studies to lower growth temperatures where clean CNTs without amorphous carbon sheaths are expected. The SEM images in Figure 1 for samples grown at temperatures ranging from 530 to 630 °C show abundant CNT growth at each of these temperatures. We find evidence for CNT growth near 520 °C (not shown); however, the results are not reproducible. No CNTs grow at 510 °C, suggesting a lower limit for this growth mechanism to be just below 530 °C. Although thermal CVD growth using Ni film catalysts does not result in vertically oriented CNTs like plasma-enhanced CVD,[17,18] observe that the structures in each image appear to be relatively straight, consistent with results from higher-temperature growth that also found exceptional diameter uniformity within a given sample. Note that the apparent similarity in the CNT diameters in each image is due to the 15−20 nm resolution limit of the SEM.

Figure 2 shows high-resolution TEM images that accurately measure the inner and outer diameters, the number of concentric walls, and allows observation of the overall crystalline quality of the CNTs. CNTs are notorious for agglomerating together into bundles when in solution; Figure 2a−e finds this to be the situation. Several bundles were imaged for each growth temperature; the images shown are representative. The study of CNTs at the edge of a bundle provides the best opportunity to observe the structure of an individual nanotube. Transmission through the center of a bundle images structures from several CNTs on top of one another, making clear identifications difficult.

Figure 2a finds the presence of single-walled nanotubes (SWNTs) with diameters of ~1.1 ± 0.2 nm on the edge of the CNT bundles grown at 530 °C. Figure 2b shows a double-walled CNT on the edge of a bundle grown at 550 °C. The inner core diameter is essentially the same as that for the SWNT measured in Figure 2a. The second wall has a diameter of ~1.8 ± 0.2 nm. Figure 2c shows an individual four-wall structure sticking out of a larger agglomeration of CNTs grown at 570 °C, with essentially the same inner wall diameter as the smaller wall structures grown at lower temperatures. Each of the four walls is evenly spaced, with the outer wall diameter measuring 3.4 ± 0.2 nm. Figure 2d,e shows CNT bundles grown at 590 and 610 °C, respectively. Identifying individual CNTs at the bundle edges is somewhat more difficult but appears to show CNTs with five and six concentric walls, all with similar inner wall diameters and evenly spaced outer walls. Finally, Figure 2f shows the best example of an individual CNT among a background of other nanotubes, grown at 630 °C. The end of the CNT in the upper left clearly shows seven concentric circles with walls emanating from each. However, this eight-wall structure has a 2.7 nm inner core diameter. The walls appear to be evenly spaced, and the outermost wall diameter is 8.0 ± 0.4 nm.

Raman Spectra. Raman spectroscopy can ascertain the nature of carbon−carbon bonding in nanocrystalline carbon materials due to the resonant enhancement of sp^2-bonded carbon atoms.[19] Figure 3 shows spectra taken for all the samples. In general, these Raman spectra are typical of that for nanocrystalline graphite (or glassy carbon) materials and consist of two well-

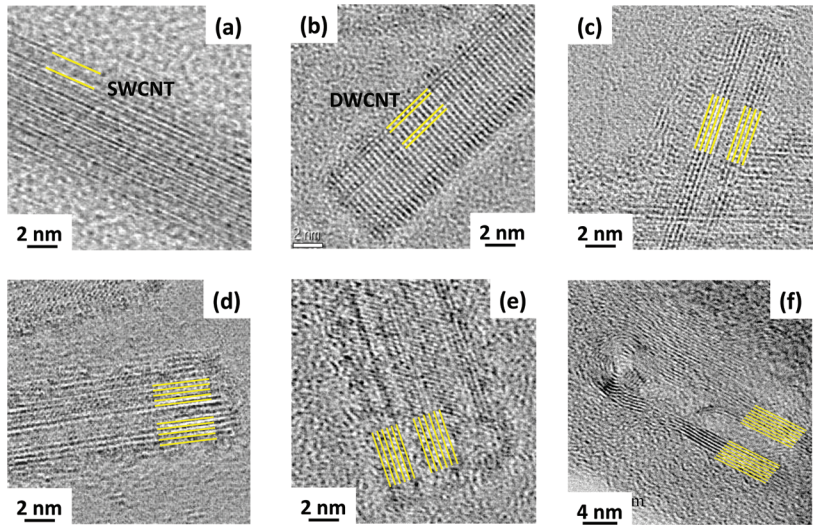

Figure 2. High-resolution TEM images from CNT bundles harvested from samples in Figure 1 grown at (a) 530, (b) 550, (c) 570, (d) 590, (e) 610, and (f) 630 °C. The lines are added as a guide to the eye to aid observation of the CNT wall structures. Note the different scale marker for (f).

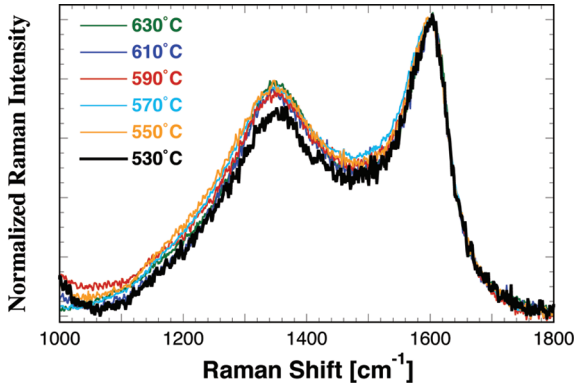

Figure 3. Raman spectra taken using 515 cm^{-1} incident light for the samples shown in Figure 1. The thick black line is from the CNTs grown at 530 °C.

known features: the G peak at ~1600 cm^{-1}, representative of graphite, and the D peak at ~1350 cm^{-1}, which represents disorder in graphene stacking planes.[20] The spectra are normalized to their G peaks and are all very similar. Just below 1000 cm^{-1} (not shown) is a broad band consisting of peaks from disordered W oxide, which results from surface oxidation of the W diffusion barrier used in these experiments and does not provide useful information about the nature of CNT growth because it most likely results from air exposure after growth.

Only the spectrum from the CNT sample grown at 530 °C (thicker black line) shows any difference, a minor reduction in the D-peak intensity. Interestingly, this is the only growth temperature for which TEM observes the growth of SWNTs. The observation of Raman spectra typical of nanocrystalline graphite for multiwalled CNTs is not surprising. The curvature of the graphene walls that form each concentric cylinder in a CNT essentially consists of small domains of disordered graphene clusters because the walls in CNTs are not known to line up with one another. Although very useful to study subtle changes in amorphous diamond-like carbon, diamond, graphite, glassy carbon, and SWNTs, Raman spectroscopy does not provide the same degree of information when studying multiwalled CNTs.[21]

Discussion

Figure 4 plots the (a) number of walls and (b) diameters of CNTs as a function of growth temperature from the TEM images

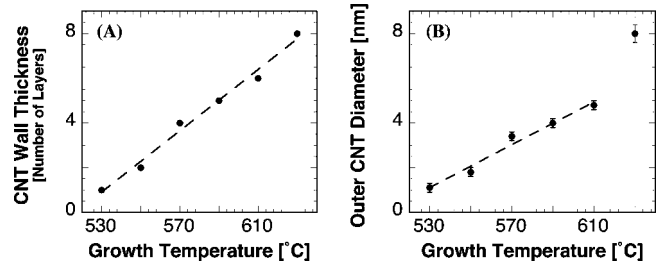

Figure 4. (A) Number of walls in CNTs as a function of growth temperature. (B) Outer CNT diameter as a function of growth temperature.

presented in Figure 2. Figure 4a shows that the CNT wall number increases linearly with growth temperature from 530 to 630 °C. Previous study at higher growth temperatures ≥ 650 °C found that diameter growth does not lead to additional graphene wall layers, but rather to the deposition of nanocrystalline graphite, or glassy carbon, sheath materials surrounding a higher-quality CNT similar to those grown at 630 °C.[16] In the lower growth temperature range of the present paper, the resulting CNTs do not exhibit any relevant degree of disordered carbon from TEM analysis. Rather, the observed CNTs appear to consist of clean, concentric walls of graphene cylinders. The images in Figure 2 demonstrate high crystalline quality multiwalled CNTs without any major observable defects, such as nanocrystalline graphite sheaths, dislocations, wall fractures, bends, kinks, bamboo features, etc., that often plague CNTs produced by other methods. Even the SEM images shown in Figure 1 find relatively straight CNTs mostly devoid of kinks and bends.

Figure 4b finds that the outer diameter increases linearly from 1.1 to 4.8 nm with increasing growth temperature up to 610 °C. CNT growth at 630 °C has a significantly larger diameter of 8.0 ± 0.4 nm and is discussed below. This linear growth behavior differs from that observed in the previous study of higher temperature growth, which found that the CNT outer diameter increases exponentially from 7 to 350 nm as the growth temperature increases from 630 to 790 °C, suggesting different mechanisms for CNT growth and nucleation at different ranges of growth temperature.[8]

It is interesting that CNTs grown at temperatures ≤ 610 °C have a similar inner core diameter of ~1.1 nm, essentially identical to that of the SWNTs grown at 530 °C. In general,

the dimension of the metal catalyst, whether nanoparticle or island, influences the CNT diameter.[22−27] The catalyst in this study is deposited as a relatively featureless 2.5 nm thick Ni film. However, every growth begins with a 600 °C treatment in a CO reducing gas for 1 h. Aside from removing oxygen from the Ni layer, the film also breaks up into islands. Because the stresses of the deposited W diffusion barrier and Ni catalyst layers are minimized, it is plausible that island formation at a given temperature is very uniform in the films.[9] Unfortunately, this is difficult to directly measure using atomic force or scanning tunneling microscopies due to the nearly immediate development of Ni oxide of such thin Ni islands upon exposure to air during sample transfer. Other groups have tried this experiment; however, at best, they can only determine trends in island diameters, not accurate measurements. However, Ni island uniformity is indirectly evidenced here by the resulting homogeneity of CNT diameters within entire samples. Given that 600 °C is near the highest temperature that experienced these growths, it is probable that the reduction anneal fixes the Ni island size from which CNT growth nucleates. This island formation at a given temperature will result in dimensionality and shape that minimizes the total free energy of the Ni surfaces and that of the W−Ni interface. The lower the initial residual stress of these metal layers, the greater the uniformity of the resulting Ni islands across a substrate surface. Higher-temperature treatment will result in larger island formation, typical of Ostwald ripening. Because the reduction anneal is near the highest temperature most of these samples experience, the Ni island size is essentially the same for all the CNTs grown at temperatures ≤ 610 °C.

Only the CNTs grown at 630 °C experience a temperature higher than the CO anneal, likely enabling the Ni islands to grow larger in size with additional ripening. These CNTs have both a significantly larger inner core diameter of 2.7 nm and a larger outer diameter than the linear functionality predicts in Figure 4b. This is consistent with the Ni island dimensionality controlling the nucleation of the inner wall of a CNT.

These results infer that the dimension of a Ni island catalyst controls the diameter of the innermost wall of a nanotube and that the temperature experienced by the hydrocarbon feed gas during thermal CVD growth controls the number of walls in a given CNT. If this hypothesis is correct, then independent control exists for the inner core diameter and the eventual number of walls in a given CNT. Only by performing the reducing anneal at lower temperatures can the Ni catalyst island size be lowered to achieve a smaller inner core diameter CNTs. Such a study is currently being pursued.

Summary

Carbon nanotubes with a high degree of crystalline perfection can grow using thermal CVD at temperatures ranging from 530 to 630 °C. The number of walls in the resulting CNTs increases linearly from one to eight over this temperature range. Using a constant 2.5 nm thick Ni catalyst layer and a constant 600 °C CO reduction temperature, the inner core diameter of the resulting CNTs essentially is constant near 1 nm, similar to the SWNTs that grow at 530 °C. As the wall number increases linearly with increasing growth temperature to 610 °C, so do the measured CNT diameters from 1 to 5 nm. This linear dependence of CNT diameter with growth temperature contrasts to the exponential thickness dependence reported earlier for growth at higher temperatures, ranging from 10 to 350 nm as the growth temperature increases from 650 to 790 °C. These results suggest a different growth mechanism for lower-temperature growth that produces significantly higher crystalline quality CNTs with controlled dimensionality.

Acknowledgment. This study was supported by the Laboratory Directed Research and Development program at Sandia National Laboratories. Sandia is a multiprogram laboratory operated by Sandia Corporation, a Lockheed Martin Company, for the United States Department of Energy's National Nuclear Security Administration under Contract No. DE-AC04-94AL85000.

References and Notes

(1) Ting, J.-M.; Wu, W.-Y.; Liao, K.-H.; Wu, H.-H. *Carbon* **2009**, *47*, 2671–2678.
(2) Okuyama, H.; Iwata, N.; Yamamoto, H. *J. Mater. Res.* **2006**, *21*, 2888–2893.
(3) Luo, Y.; Wal, R. V.; Hall, L. J.; Scherson, D. A. *Electrochem. Solid-State Lett.* **2003**, *6*, A56–A58.
(4) Park, J.-B.; Cho, Y.-S.; Hong, S.-Y.; Choi, K.-S.; Kim, D.; Choi, S.-Y.; Ahn, S.-D.; Song, Y.-H.; Lee, J.-H.; Cho, K.-I. *Thin Solid Films* **2002**, *415*, 78–82.
(5) Lee, C. J.; Park, J. H.; Park, J. *Chem. Phys. Lett.* **2000**, *323*, 560–565.
(6) Lee, C. J.; Park, J.; Kim, J. M.; Huh, Y.; Lee, J. Y.; No, K. S. *Chem. Phys. Lett.* **2000**, *327*, 277–283.
(7) Zhang, X.; Cao, A.; Wei, B.; Li, Y.; Wei, J.; Xu, C.; Wu, D. *Chem. Phys. Lett.* **2002**, *362*, 285–290.
(8) Siegal, M. P.; Overmyer, D. L.; Provencio, P. P. *Appl. Phys. Lett.* **2009**, *80*, 2171–2173.
(9) Siegal, M. P.; Overmyer, D. L.; Kaatz, F. H. *Appl. Phys. Lett.* **2004**, *84*, 5156–5158.
(10) Baker, R. T. K.; Barber, M. A.; Harris, P. S.; Feates, F. S.; Waite, R. J. *J. Catal.* **1972**, *26*, 51–62.
(11) Cantoro, M.; Hofmann, S.; Pisana, S.; Scardaci, V.; Parvez, A.; Ducati, C.; Ferrari, A. C.; Blackburn, A. M.; Wang, K.-Y.; Robertson, J. *Nano Lett.* **2006**, *6*, 1107–1112.
(12) Hofmann, S.; Blume, R.; Wirth, C. T.; Cantoro, M.; Sharma, R.; Ducati, C.; Havecker, M.; Zafeiratos, S.; Schnoerch, P.; Oestereich, A.; Teschner, D.; Albrecht, M.; Knop-Gericke, A.; Schlogl, R.; Robertson, J. *J. Phys. Chem. C* **2009**, *113*, 1648–1656.
(13) Hofmann, S.; Sharma, R.; Ducati, C.; Du, G.; Mattevi, C.; Cepek, C.; Cantoro, M.; Pisana, S.; Parvez, A.; Cervantes-Sodi, F.; Ferrari, A. C.; Dunin-Borkowski, R.; Lizzit, S.; Petaccia, L.; Goldoni, A.; Robertson, J. *Nano Lett.* **2007**, *7*, 602–608.
(14) Nessim, G. D.; Hart, J.; Kim, J. S.; Acquaviva, D.; Oh, J.; Morgan, C. D.; Seita, M.; Leib, J. S.; Thompson, C. V. *Nano Lett.* **2008**, *8*, 3587–3593.
(15) Kim, C.-K.; Kang, J.-T.; Ryu, H.-W.; Lee, I.-S.; Park, J.-H.; Lee, C.-S.; Lee, E.-W.; Lee, J.-R. *Jpn. J. Appl. Phys.* **2008**, *47*, 4803–4806.
(16) Siegal, M. P.; Miller, P. A.; Provencio, P. P.; Tallant, D. R. *Diamond Relat. Mater.* **2007**, *16*, 1793–1798.
(17) Ren, Z. F.; Huang, Z. P.; Xu, J. W.; Wang, J. H.; Bush, P.; Siegal, M. P.; Provencio, P. P. *Science* **1998**, *282*, 1105–1107.
(18) Huang, Z. P.; Xu, J. W.; Ren, Z. F.; Wang, J. H.; Siegal, M. P.; Provencio, P. P. *Appl. Phys. Lett.* **1998**, *73*, 3845–3847.
(19) Siegal, M. P.; Tallant, D. R.; Martinez-Miranda, L. J.; Barbour, J. C.; Simpson, R. L.; Overmyer, D. L. *Phys. Rev. B* **2000**, *61*, 10451–10462.
(20) Friedmann, T. A.; McCarty, K. F.; Barbour, J. C.; Siegal, M. P.; Dibble, D. C. *Appl. Phys. Lett.* **1996**, *68*, 1643–1645.
(21) Dresselhaus, M. S.; Dresselhaus, G.; Saito, R.; Jorio, A. *Phys. Rep.* **2005**, *409*, 47–99.
(22) Merkulov, V. I.; Lowndes, D. H.; Wei, Y. Y.; Eres, G.; Voelkl, E. *Appl. Phys. Lett.* **2000**, *76*, 3555–3557.
(23) Lee, C. J.; Lyu, S. C.; Cho, Y. R.; Lee, J. H.; Cho, K. I. *Chem. Phys. Lett.* **2001**, *341*, 245–249.
(24) Chhowalla, M.; Teo, K. B. K.; Ducati, C.; Rupesinghe, N. L.; Amaratunga, G. A. J.; Ferrari, A. C.; Roy, D.; Robertson, J.; Milne, W. I. *J. Appl. Phys.* **2001**, *90*, 5308–5317.
(25) Cheung, C. L.; Kurtz, A.; Park, H.; Lieber, C. M. *J. Phys. Chem. B* **2002**, *106*, 2429–2433.
(26) Wang, S. G.; Zhang, Q.; Yoon, S. F.; Ahn, J. *Scr. Mater.* **2003**, *48*, 409–412.
(27) Wright, A. C.; Xiong, Y.; Maung, N.; Eichhorn, S. J.; Young, R. J. *Mater. Sci. Eng., C* **2003**, *23*, 279–283.

JP105815U